

Oxide Scale Adhesion and Impurity Segregation at the Scale/Metal Interface

Peggy Y. Hou* and John Stringer†

Received April 22, 1992; revised June 29, 1992

The chemistry at scale/metal interfaces was studied using scanning Auger microscopy after removal of the scale in ultra-high vacuum using an in situ scratching technique. Al_2O_3 and Cr_2O_3 scales formed between 900°C and 1100°C on Fe-18 wt.% Cr-5 wt.% Al and on Ni-25 wt.% Cr alloys, respectively, were investigated. The adhesion of these scales was determined qualitatively by way of micro-indentation and scratching on the surface oxide. All of the alumina scales fractured to the same degree to expose the metal surface, regardless of the oxidation temperature. The chromia-forming alloy on the other hand, developed more adherent scales at lower oxidation temperatures. About 20 at.% sulfur was found at the metal surface in all cases, and its presence was not only detected on interfacial voids, but also on areas where the scale was in contact with the alloy at temperature. Results from this study clearly demonstrated that sulfur as an alloying impurity does segregate to the scale/alloy interface. However, for alumina scales and chromia scales, the effect of this segregation on oxide adhesion is noticeably different.

KEY WORDS: sulfur segregation; scale adhesion; Al_2O_3 scale; Cr_2O_3 scale; scale/alloy interface; scratch adhesion test; micro-indentation.

INTRODUCTION

The protection of high temperature alloys and coatings against oxidation is provided by the formation of slow-growing oxide films which often contain Al_2O_3 and/or Cr_2O_3 . One major factor inhibiting the protection is the tendency of the oxides to break away from the metal surface, or spall, under

*Materials Sciences Division, Lawrence Berkeley Laboratory, Berkeley, California 94720.

†Electric Power Research Institute, Palo Alto, California 94304.

thermal cycling conditions. The degree of spallation depends on many factors: the specific oxide growth mechanism, the stresses in the oxide-metal system, the ability of the system to relieve such stresses, and the fracture resistance of the oxide, the metal and the scale/metal interface. The strength of the oxide/alloy interface found on Al_2O_3 - and Cr_2O_3 -forming alloys is traditionally recognized as being weak, unless the alloy also contains minor amounts of a reactive element, such as Y, Ce or Hf, or fine dispersions of its oxide.¹ A weak interface is perceived because these oxide scales are poorly adherent and separate easily from the metal substrate. However, in recent years, several investigators²⁻⁴ have suggested independently that these interfaces are in fact intrinsically strong, but are weakened by an impurity such as sulfur which segregates from the bulk of the alloy to the interface.

Although segregation of sulfur to alloy surfaces has been repeatedly demonstrated with *in situ* heating in a vacuum chamber,^{3,5-8} a clear indication that sulfur or other impurities are present at the scale/metal interface of non-adherent oxide scales is lacking. Recently, Grabke and co-workers⁹ using AES depth profiling techniques have concluded that there is no equilibrium segregation of sulfur to the metal/oxide interface. From thermodynamic considerations, the size and charge effect of a sulfur atom at the metal/oxide interface would make the segregation process impossible. Instead, the authors believe that the adverse effect of sulfur on scale adhesion is the result of more favorable void formation at the interface, since sulfur segregation to the surface of voids would lower their surface energy. However, our preliminary work¹⁰ using an *in situ* scratch device in the high vacuum chamber of a scanning auger microprobe indicted a sulfur presence at the scale/alloy interface, but the amount of sulfur was very low due to large amounts of oxygen and carbon adsorption at the metal surface. The purpose of this study is to further investigate the chemistry at the alloy surface after the oxide scale had been removed in better vacuum conditions, and to relate this to the adhesion property of the scale.

EXPERIMENTAL METHODS

An alumina-forming Fe-18 wt.% Cr-5 wt.% Al and a chromia-forming Ni-25 wt.% Cr alloy were made by induction melting and casting from high purity materials under an argon atmosphere. The ingots were subsequently homogenized in vacuum at 1100°C for 24 hr. Both alloys are single-phased. The average grain size for the Ni-25Cr was 1.5 mm × 0.4 mm × 0.3 mm and for the Fe-18Cr-5Al was 0.83 mm × 0.48 mm × 0.48 mm. The actual composition of both alloys was similar to the intended one. Results from chemical

Table I. Chemical Analysis of Alloys

Alloy	Fe	Ni	Cr	Al	S	C
Fe-18Cr-5Al	Bal.	—	18.25 wt.%	4.73 wt.%	130 ppm	30 ppm
Ni-25Cr	0.03 wt.%	Bal.	24.93 wt.%	—	80 ppm	20 ppm

analysis are shown in Table I. Specimens 15 mm × 10 mm × 1 mm were cut from only the center of the homogenized ingots to avoid surface contaminants. Prior to the oxidation treatments the specimens were ground to a 1200 SiC finish and ultrasonically cleaned.

Oxidation tests were carried out in dry oxygen at 1 atm total pressure in a horizontal tube furnace. Al₂O₃ and Cr₂O₃ scales were formed between 900°C and 1100°C. The oxidation duration was chosen such that the same type of scale formed at different temperatures would develop a similar thickness, and there would be little spallation during cooling. Specimens in alumina crucibles were first placed at one end of a closed mullite reaction tube while the system was being equilibrated with flowing oxygen. Oxidation was initiated by pushing the crucibles into the hot zone of the furnace. After the desired time, the crucibles were quickly removed from the furnace and capped, and the specimens were allowed to cool to room temperature in air.

A qualitative indication of scale adhesion was obtained by comparing the degree of through scale fracture caused by a scratch or a micro-indent made on the surface of the oxidized specimen.¹¹⁻¹³ The effect of the indentation and the morphology of the scale and the underlying alloy were subsequently determined using a scanning electron microscope (SEM). The chemistry at the scale/metal interface was studied using scanning Auger microscopy (SAM) after removal of the scale in ultra-high vacuum (UHV) using an *in situ* scratching technique.

The apparatus used for the *in situ* scratching experiments has been described in detail elsewhere.¹⁰ The device is attached to the UHV chamber of a PHI model 660 scanning Auger microprobe, but is normally isolated from the UHV by a gate valve. The main body of the device is a long rod, and mounted on its end are several common indenter tips. The rod can be pushed into the UHV chamber once the device has been pre-pumped and the gate valve is opened. Using the built-in SEM of the SAM, an indenter can be placed directly above the specimen surface. Scratching or indentation of the specimen is accomplished by manipulating the specimen stage control of the SAM, while the rod, and the indenter, stay stationary. A pair of strain gauges mounted on the rod then indicate the level of load during a scratch or an indent. Loads ranging from 200 to 1000 grams were usually used on an oxidized specimen using a Vickers tip.

RESULTS

Oxidation Behavior

The oxidation behavior of all the tested specimens is summarized in Table II. The oxide scale formed on the Fe-18Cr-5Al alloy was identified by X-ray diffraction to be α - Al_2O_3 , and it is single-layered. By choosing different oxidation durations, the alumina scales formed at different temperatures developed very similar thickness. Measurements of scale thickness under the SEM on cross-sectioned specimens showed that its average was $1.1 \mu\text{m}$. This thin oxide showed no spallation during cooling; this was verified not only by weight measurements but also by extensive observations made under the SEM.

The Ni-25Cr alloy oxidized under the conditions given in Table II developed a single-layered scale of Cr_2O_3 . The 24-hr oxide formed at 900°C , the 4-hr oxide at 1000°C and the 1-hr oxide at 1100°C were the closest in thickness, and cross-sectional measurements showed that to be approximately $2.8 \mu\text{m}$. Although having a similar thickness, the degree of scale spallation was higher with higher oxidation temperatures.

Scale Fracture Behavior and Interfacial Chemistry

Al₂O₃ Scale

Indentations made on the surface of a thin film have been known to induce film delamination, if the interfacial area is the weakest region of the film/substrate structure.¹³ The delamination process is driven by the misfit of material which was displaced by the indent impression. Such delamination was observed with the thermally grown alumina scales studied here. Indentations made on the oxidized surface always caused decohesion of the scale from the underlying alloy. The area which was separated could be easily

Table II. Summary of Alloy Oxidation Behavior

Alloy type	Temperature ($^\circ\text{C}$)	Duration	Total wt. gram (mg/cm^2)	Spalled oxide (mg/cm^2)
Fe-18Cr-5Al	900	120 hr	0.094	0
	1000	3 hr	0.097	0
	1100	15 min	0.091	0
Ni-25Cr	900	24 hr	0.35	0
	1000	4 hr	0.52	0.06
	1100	1 hr	0.48	0.14
	1000	10 min	0.09	0
	1000	1 hr	0.18	0

observed using polarized light, as seen in Fig. 1. The scales in Figs. 1a and 1b were formed at 900°C and 1100°C, respectively, with an equal thickness. Upon indentation, the area of decohesion in both cases was found to be very similar. The failure of alumina scales, in terms of delaminations caused by different loads of indents, in relation to the oxidation temperatures at which these scales were formed is illustrated in Fig. 2. From here, it is clear that the area of delamination was directly related to the indentation load, and within experimental scatter, scale decohesion caused by an indent was independent of the oxidation temperature.

The SEM image of an indentation mark made on a 1100°C alumina scale is shown in Fig. 3a. The delaminated area is seen to consist of oxide which was either detached or spalled off from the substrate. Using a piece of adhesion tape, the detached oxide could be easily removed to reveal large areas of the underlying alloy surface, as seen in Fig. 3b. Major portions of this alloy surface had a rough appearance which resemble regions where the metal was in contact with the oxide at temperature, so that the roughness was a result of oxide imprint. A number of smooth areas were also apparent; most, but not all, were found along the initial polishing marks on the specimen surface. These voids have often been considered as areas where the scale had lost contact with the metal at temperature. The density of such voids was noticeably less with scales grown at 1000°C, and became very low when oxidation was performed at 900°C (Fig. 4). Careful examination of Fig. 4 reveals that most of the "ridge-like" oxides on the specimen surface actually resulted from substrate deformation rather than oxide buckling.

The large areas of oxide delamination made studying the chemistry of the $\text{Al}_2\text{O}_3/\text{FeCrAl}$ interface easy. Figures 5a and b show two interfacial areas exposed under ultra high vacuum by *in situ* scratching. Again, the uncovered areas are comparable in size, which further demonstrates that scale failure was not related to the oxidation temperature. Scratching was used here instead of indentation because the dragging motion caused more scale fragments to come off, thus exposing greater areas for subsequent Auger analyses.

The areas marked on Figs. 5a and b were analyzed by Auger electron spectroscopy (AES). In all cases, regardless of the oxidation temperature or the interfacial morphology, i.e., oxide-imprints vs voids, the chemistry of these surfaces was identical. A typical AES survey of these areas is shown in Fig. 5c. The sulfur content was calculated to be 19 at.% using tabulated standardless Auger sensitivity factors. An extremely low oxygen signal indicated that the alloy surface was not exposed to air; in other words, the scale above the alloy surface was in intimate contact until the scratching took place under UHV. As expected from oxide growth, the alloy surface was depleted in aluminum, but enriched in chromium. However, about 20 at.%

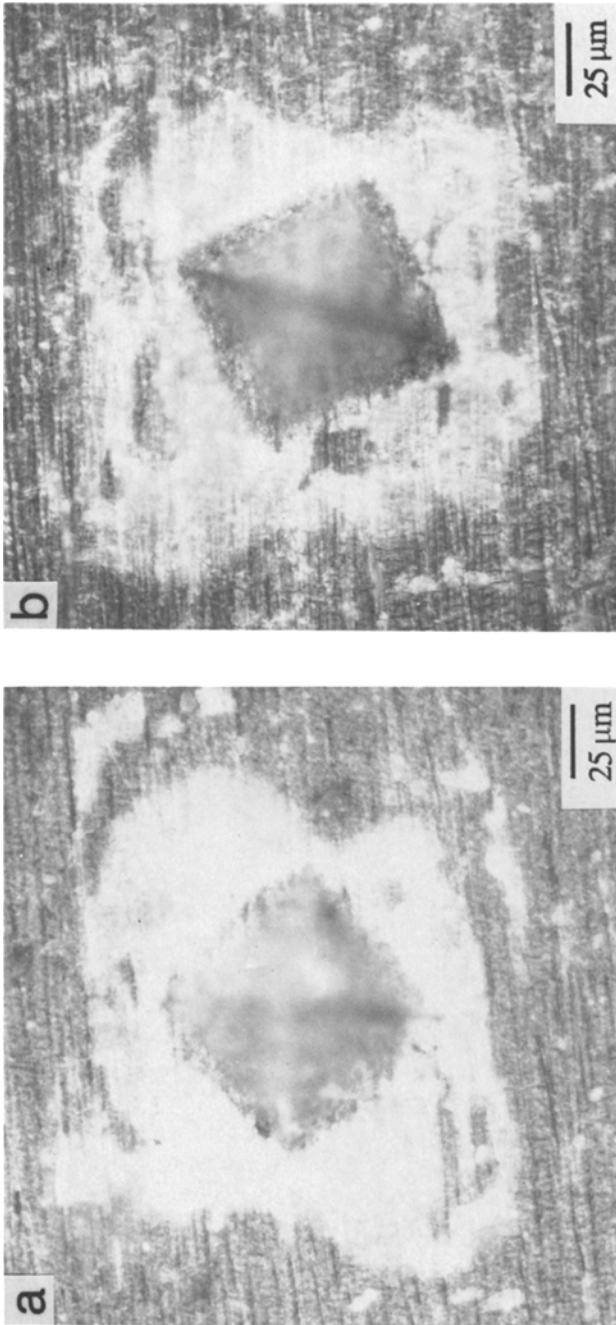


Fig. 1. Optical micrographs under polarized light showing the interfacial fractures caused by micro-indentations. The indents (1000 g in both cases) were made through an approximately 1- μm thick Al_2O_3 scale on a Fe-18Cr-5Al alloy. The scale was formed at (a) 900°C for 120 hr, and (b) 1100°C for 15 min.

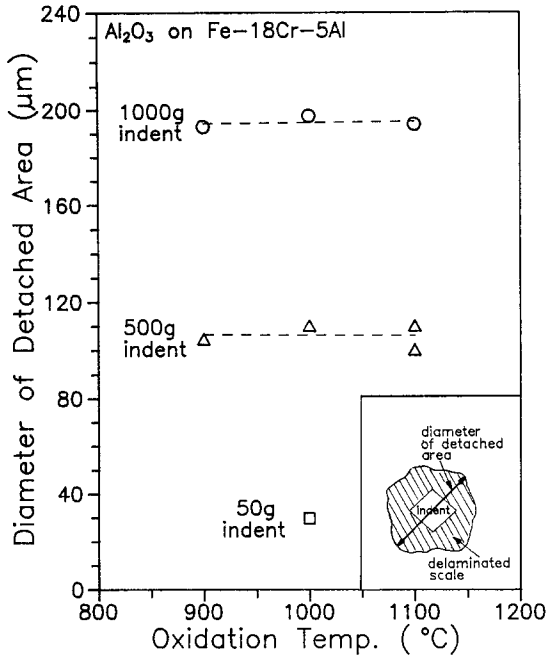


Fig. 2. The degree of indent-induced scale delamination as a function of oxidation temperature. The "diameter of detached area" was measured from one point of the delamination to the other along a line normal to the edges of the indentation diamond, as illustrated in the insert. All alumina scales were of similar thickness: approximately $1 \mu\text{m}$.

carbon was also detected, and it is important to determine whether this carbon came as a result of surface contamination from the vacuum or was indeed present at the scale/alloy interface before scale removal. Both the sulfur and the carbon were concentrated only at the metal surface. Their concentration quickly dropped upon sputtering, and became zero after about 6 nm. Because of this narrow range and the roughness of the oxide surface and the interface, depth profiling using argon gas through the surface of these oxide scales was usually unable to detect the presence of such segregated impurities at the interface.

To verify the source of carbon found on the metal side of the $\text{Al}_2\text{O}_3/\text{FeCrAl}$ interface, the build up of oxygen and carbon, which are the most common residual species in a UHV chamber other than hydrogen, on a freshly-exposed alloy surface was monitored with time. Results are shown in Fig. 6 where time zero represents the time when the scratch was made. A fast oxygen build up was observed which could be easily extrapolated to

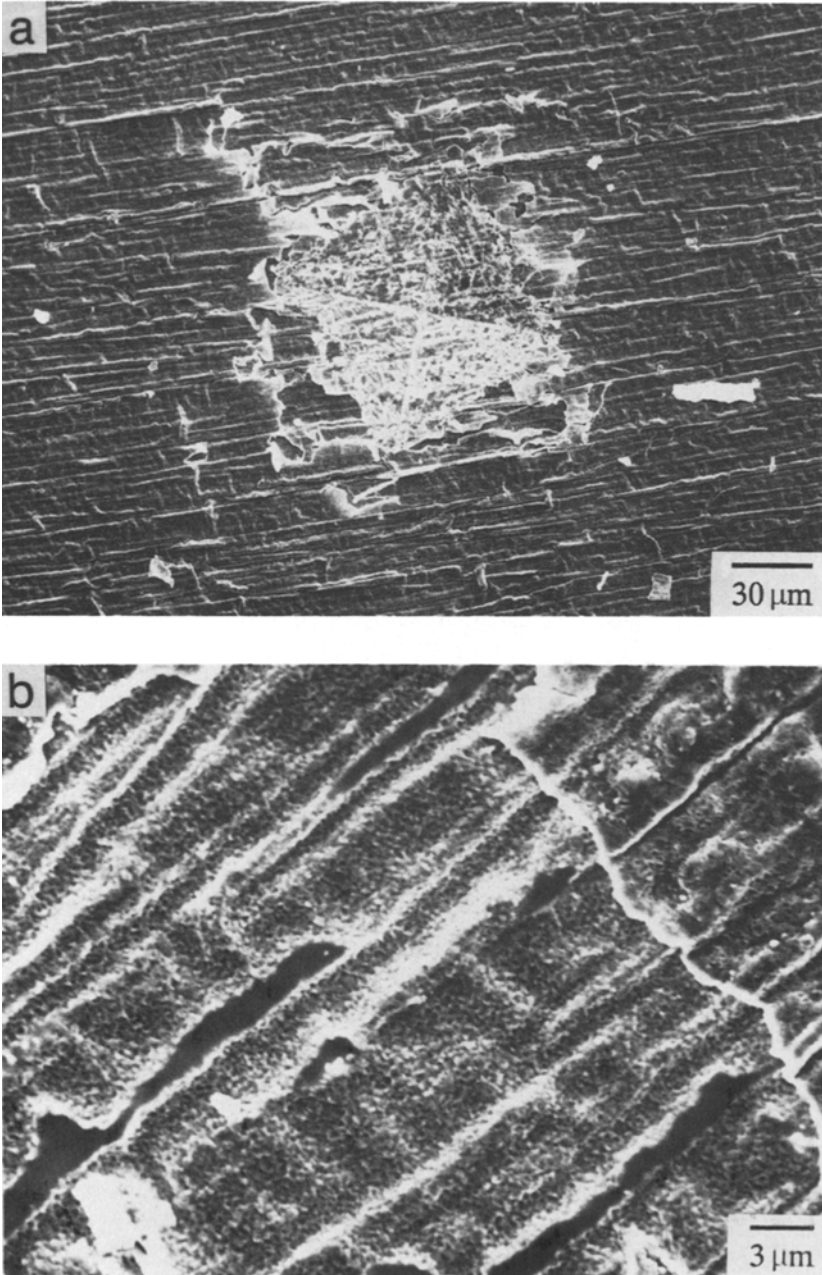


Fig. 3. (a) SEM micrograph of a 1000-g indent made on the alumina scale formed on Fe-18Cr-5Al at 1100°C for 15 min. (b) Magnified view of the alloy surface after removal of detached scales using a piece of adhesive tape.

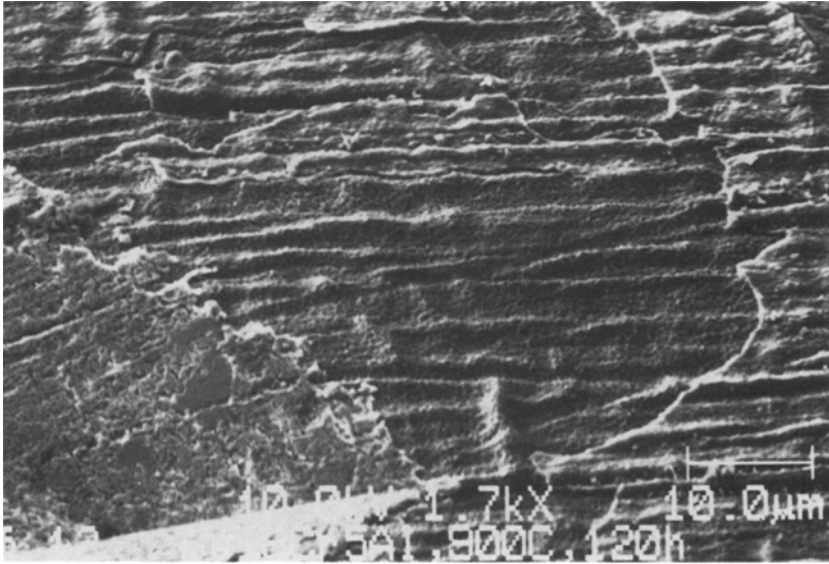


Fig. 4. SEM micrograph showing the area around a 1000-g indent made on an alumina scale formed at 900°C for 120 hr. Detached scale fragments had been peeled off with a piece of adhesion tape.

zero at the time of scratch. The build up of carbon was slower and an extrapolation to time zero shows a finite amount which correspond to about 15%. If the chamber pressure were higher during the scratch, the amount of carbon and oxygen would be higher than that shown here. Figure 7 compares the amount of carbon found as a function of chamber pressure at the time the scratches were made. With both the alumina-former and the chromia-former, the amount of carbon increased exponentially with poorer vacuum. Extrapolating the data points for Ni-25Cr, one would expect no carbon on the metal surface below a vacuum of 10^{-9} torr. However, under the same condition, about 15% carbon would be found on the Fe-18Cr-5Al surface, which is consistent with the carbon build up result shown in Fig. 6. These results indicated that a carbon content similar to that of sulfur was present on the Fe-Cr-Al surface beneath the alumina scale.

Cr₂O₃ Scale

With chromia scales, indent-induced delamination was optically unresolvable because of the scales' opaqueness. However, spallation of detached oxides usually occurred to expose the underlying alloy which could be easily detected due to its high reflectivity. Figure 8 compares the effect of a 1000 g

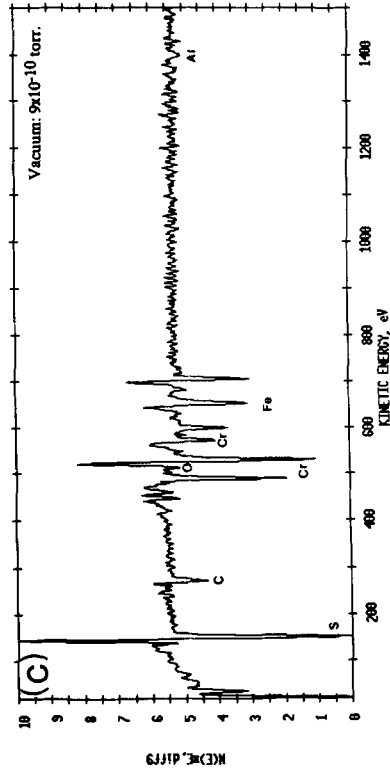
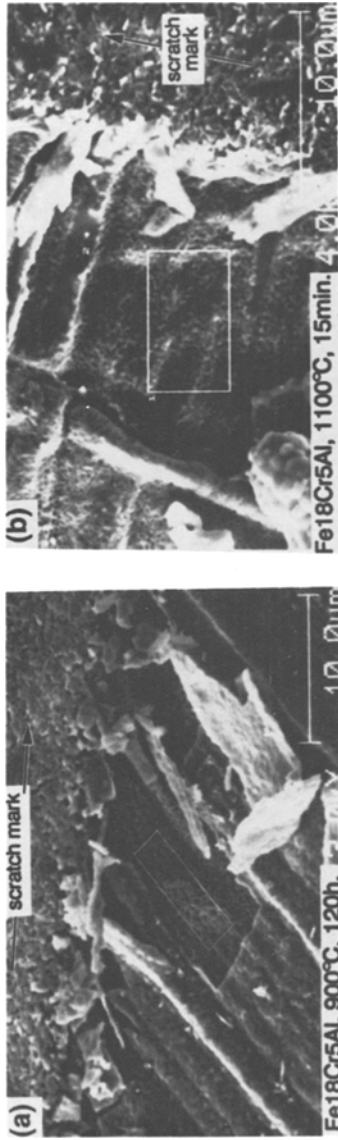


Fig. 5. SEM micrographs of scratch-induced scale fractures. The alumina scale was formed at (a) 900°C for 120 hr, and (b) 1100°C for 15 min. Scratches were made with a diamond stylus in ultra-high vacuum. The marked areas on both micrographs indicate regions on which Auger analyses were made, and (c) is a typical Auger spectrum of the tested area.

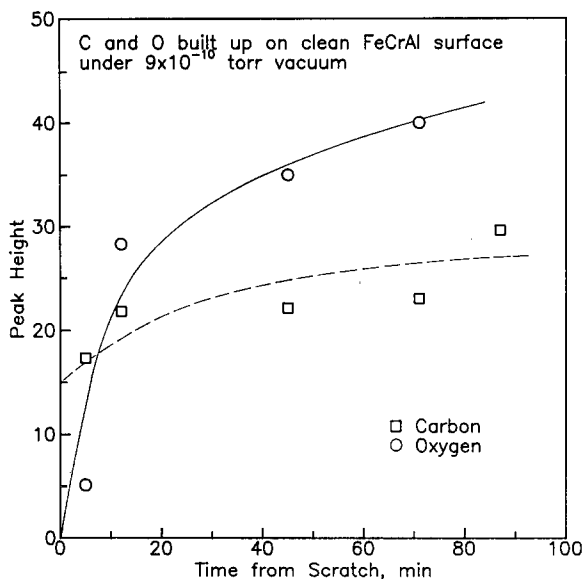


Fig. 6. Carbon and oxygen build up on Fe-18Cr-5Al alloy surface under 9×10^{-10} torr vacuum after the removal of surface alumina scale by *in situ* scratching.

indent made on chromia scales which were grown at two different temperatures. On the 1000°C scale (Fig. 8b), a number of bright spots appeared as a result of the indentation, but the 900°C scale (Fig. 8a) showed no such behavior. After pressing a piece of adhesive tape around the indented area, a few more extra bright spots appeared on the 1000°C scale, but again, the 900°C scale remained totally opaque. Figure 9 shows SEM micrographs of a 10-min chromia scale formed at 1000°C before and after a 500 g indent. The scale was only about $1 \mu\text{m}$ thick. Indent-induced fractures preferentially occurred at buckled oxides, most of which appeared along initial 600-grit scratch marks on the specimen surface. Beneath these buckles were voids at the interface, and no oxide-imprinted areas were found. With the 900°C scale, as seen in Fig. 10, only a few small areas of oxide loss occurred and they either appeared above an interfacial void, or within the oxide scale. The Cr_2O_3 scale formed at this lower temperature was much smoother, with no apparent oxide buckles. Furthermore, the oxide around the indent did not show any cracks nor did it appear damaged by the process. This behavior was very different from that shown in Fig. 3 for the alumina scales.

While indentations on chromia scales only resulted in localized scale failure above interfacial voids, scratches were more effective in removing

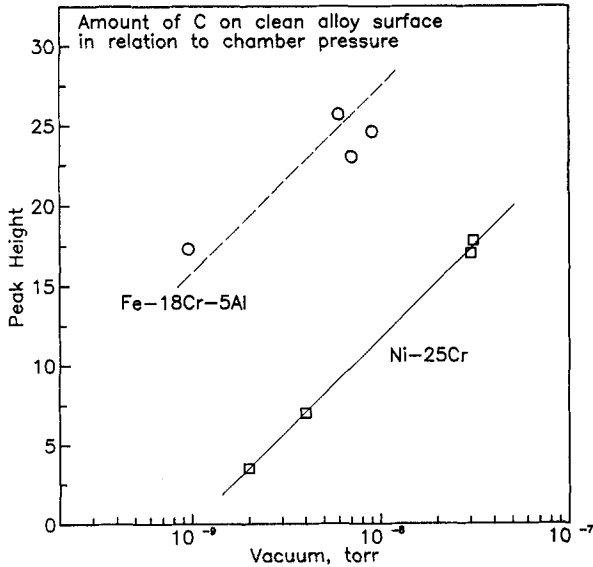


Fig. 7. Amount of carbon on the alloy side of scale/alloy interfaces in relation to vacuum condition at the time of scale/alloy separation. The carbon content was determined by Auger electron spectroscopy about five minutes after the layer of oxide scale had been removed by *in situ* scratching.

larger pieces of oxides. Figure 11 shows SEM micrographs of some scratch-induced fractures. These scales were all scratched in UHV, followed by AES analyses of the exposed metal surfaces. Areas on those micrographs marked with numbers have all been analyzed, and these results will be discussed shortly. Three different scales, which were oxidized at different temperatures but with a similar thickness, were compared. For the 900°C oxide, fractures occurred partly within the scale and partly at the scale/metal interface. Again, most of the alloy surfaces exposed by scale fractures were voids, as seen in Figs. 11a and b. Only occasionally would a small oxide-imprinted area next to a void be found. Scales that formed at 1000°C fractured mainly at the interface, exposing not only voids, but also small areas of oxide imprints. With thinner scales however, scale failure would still only occur above interfacial voids. The chromia scale grown at 1100°C had the highest degree of spallation upon scratching. In this case, the fractures occurred entirely at the scale/alloy interface showing nearly equal areas of voids and oxide imprints. This scale also had the highest degree of convolution as seen in Fig. 11d.

From the micrographs shown in Figs. 9–11, it is seen that the degree of scratch or indent-induced fractures depended heavily on the oxidation

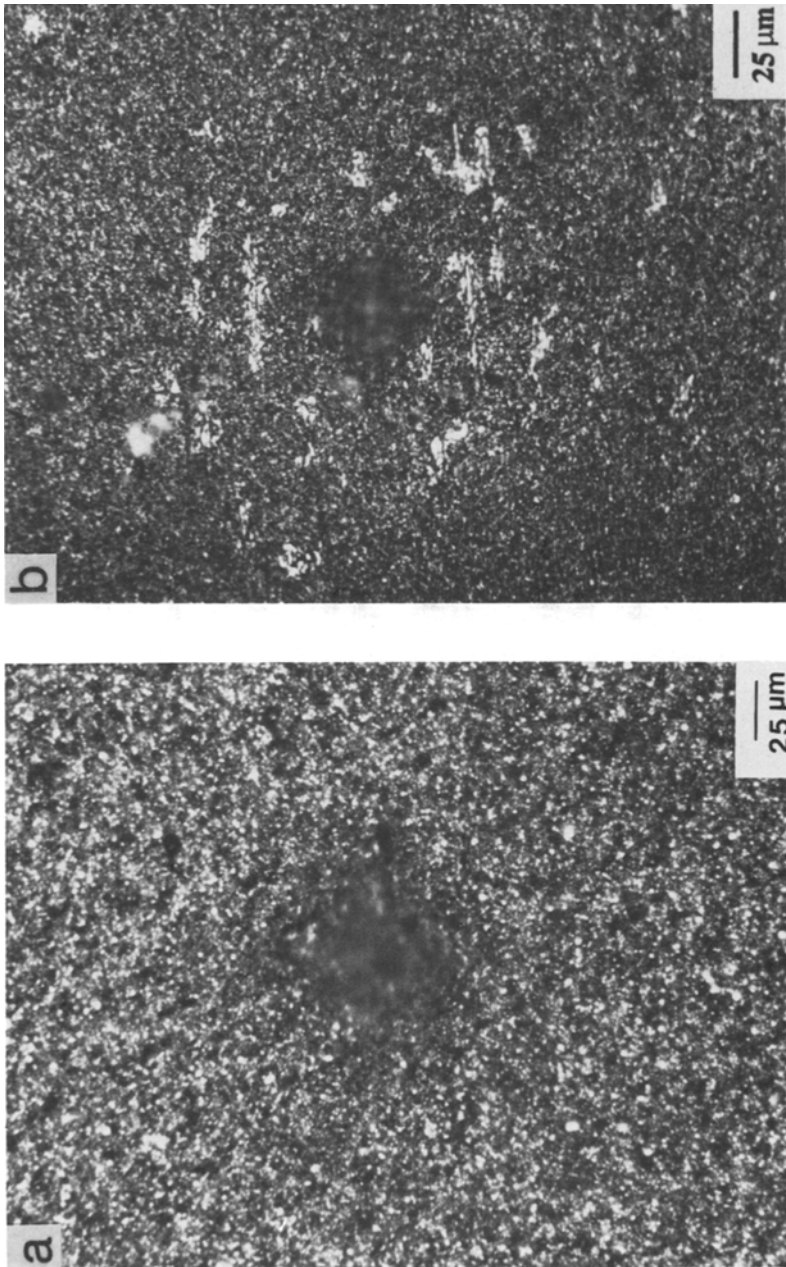


Fig. 8. Optical micrographs showing the effect of a 1000-g load indentation made through approximately 2- μ m thick chromia scales on Ni-25Cr. The scales were formed at (a) 900°C for 24 hr, and (b) 1000°C for 1 hr.

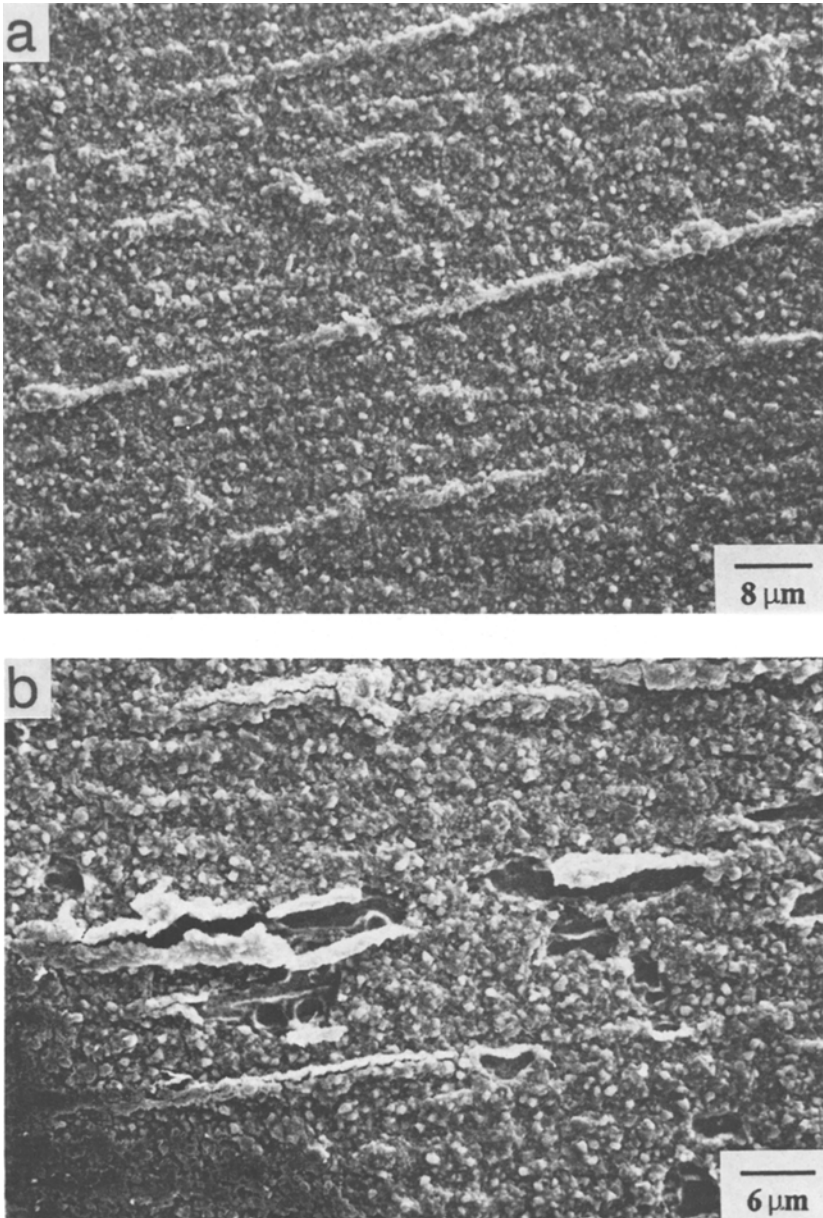


Fig. 9. SEM micrographs of Cr_2O_3 scale (a) before, and (b) after a 500-g indentation. The scale was formed on Ni-25Cr at 1000°C for 10 min.

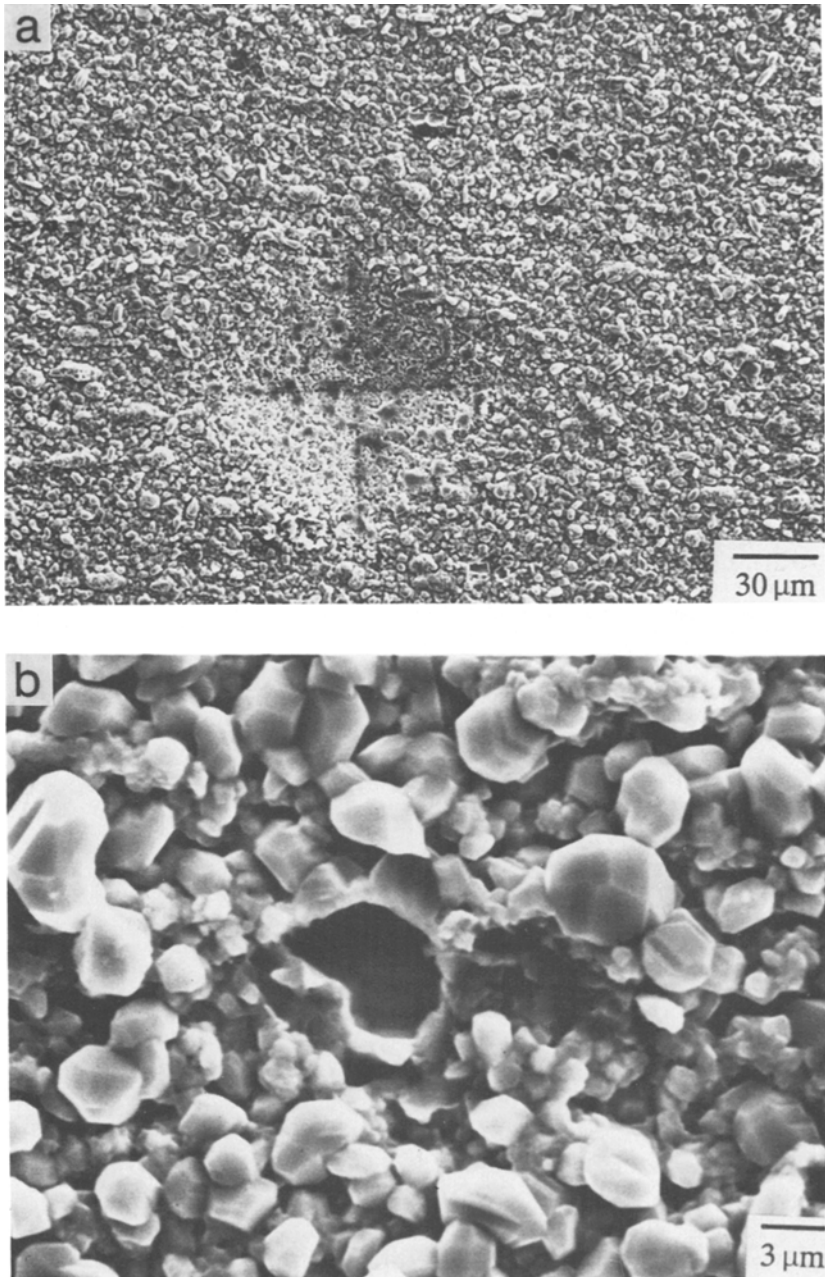


Fig. 10. SEM micrographs of Cr_2O_3 scale formed at 900°C for 24 hr. (a) Area around a 1000-g indentation, and (b) magnified view of indent-induced scale fracture.

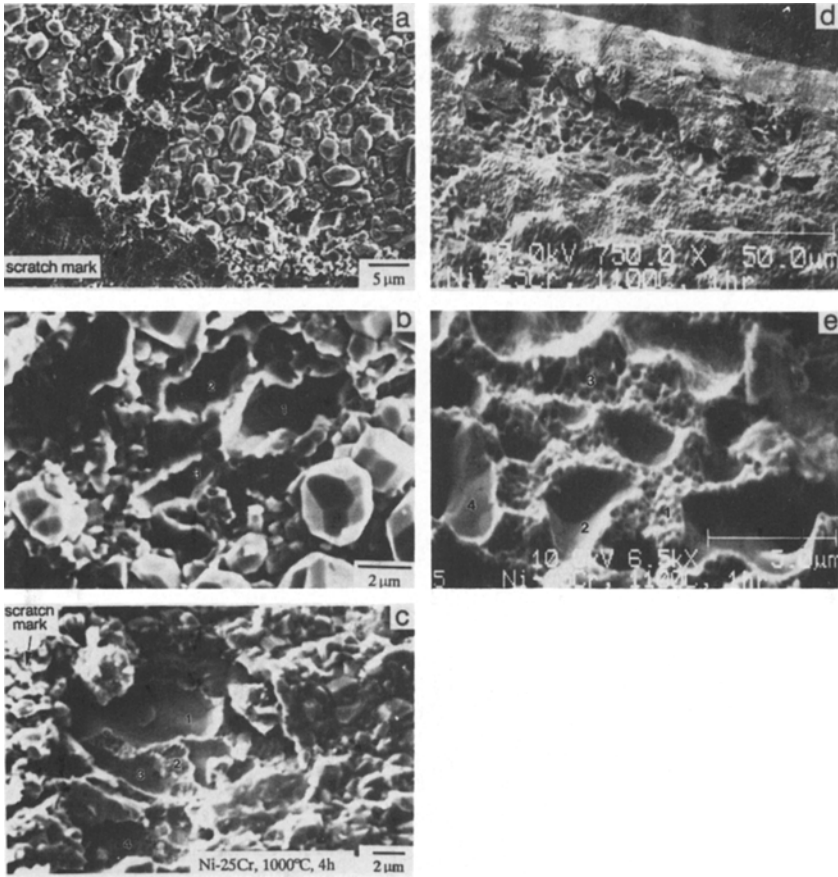


Fig. 11. SEM micrographs of scratch-induced scale fractures. The oxidation conditions were (a) and (b) 900°C for 24 hr, (c) 1000°C for 4 hr. and (d) and (e) 1100°C for 1 hr.

temperature. An attempt was made to quantify this dependence by plotting in Fig. 12 the area of exposed metal surface caused by a 800 g scratch against oxidation temperatures. Unlike the case of alumina scales grown on Fe-Cr-Al (Fig. 2), where scale failure was not affected by oxidation temperatures, the response here is nearly exponential, with much greater failure found at higher temperatures.

Whether the exposed interface was a smooth void or a rough oxide imprint, and regardless of the temperature at which the oxides were formed, a very distinct sulfur signal was found on these surfaces. A typical example is given in Fig. 13. The alloy surface beneath the scale contained about 17

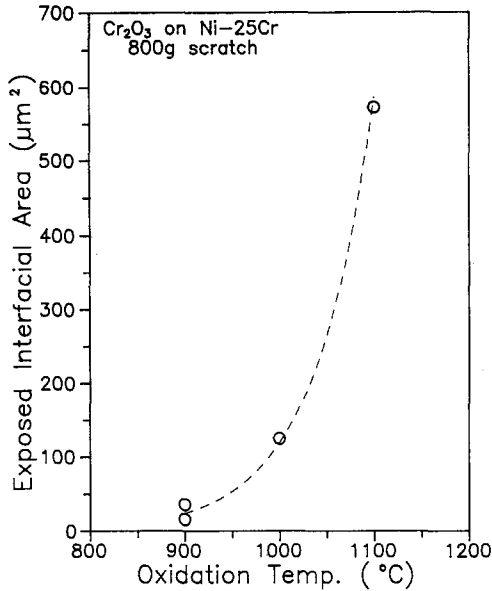


Fig. 12. The relationship between scratch-induced interfacial failure and oxidation temperatures of chromia scales formed on Ni-25Cr. All scales were approximately $2.8 \mu\text{m}$ in thickness.

at.% sulfur and was rich in nickel and poor in chromium. Much less carbon was present here than on the Fe-Cr-Al surface shown in Fig. 5c, even though the vacuum condition in this case was poorer. The extremely low oxygen signal again demonstrated that the alloy surface was not in contact with air before *in situ* scratching. Sulfur was found only at the surface to a depth of approximately 4 nm.

DISCUSSION

One of the objectives of this work was to determine if sulfur was indeed present at the scale/alloy interface after oxidation. Using oxide scales which did not show extensive spontaneous spallation during cooling, followed by scratch removal of the scale under high vacuum conditions, the presence of sulfur at scale/alloy interfaces was clearly demonstrated using Auger electron microscopy. Between the oxidation temperatures of 900°C and 1100°C, about 17-19 at.% sulfur was found at the metal side of the interface on Fe-18Cr-5Al, which formed alumina scales, and on Ni-25Cr, which formed chromia scales. Numerous areas of voids and oxide imprints were analyzed,

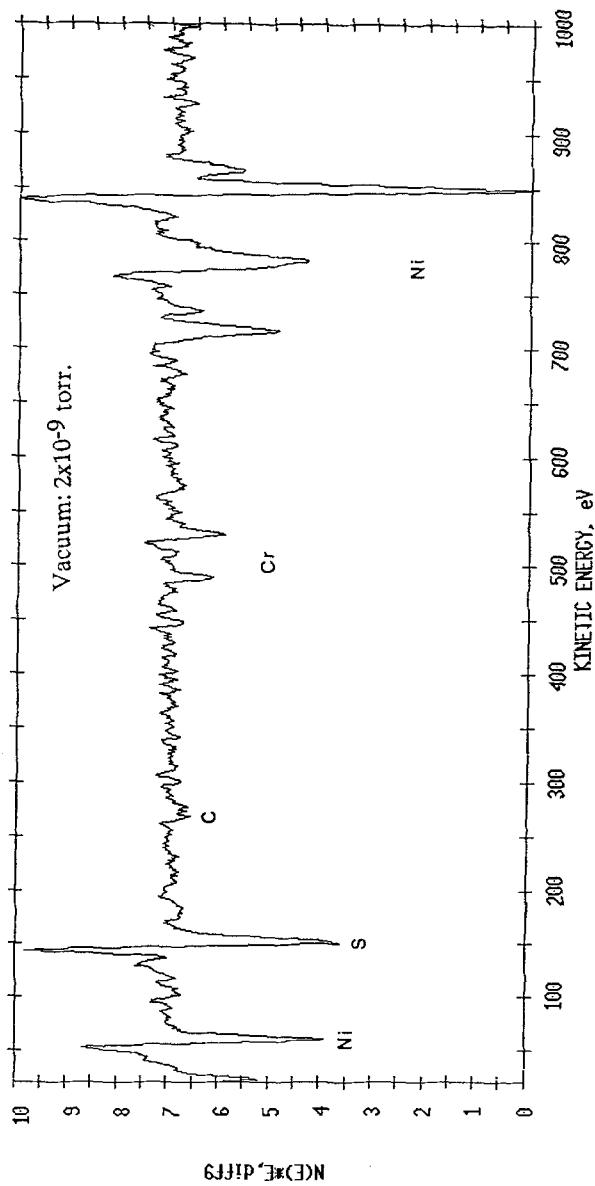


Fig. 13. Typical Auger analysis of marked areas in Figs. 9b, c, and e.

and the amount of sulfur was found to be nearly the same in all cases. Its presence was independent of the oxidation temperature or the interfacial morphology, and it was heavily concentrated at the alloy surface, within about 4–6 nm.

The fact that near zero amounts of oxygen were detected on the exposed alloy surfaces proves that the oxide scale was not separated from the alloy prior to the scratch process. In other words, the scale was in intimate contact with the alloy surface until its exposure in vacuum, so scale/alloy separation did not precede sulfur segregation, as the argument presented by Grabke *et al.*⁹ may suggest. With thicker scales, which had undergone longer oxidations and showed heavier spallation during cooling, some alloy surfaces had been found with less sulfur, but a very high oxygen content.¹⁰ In those instances, the scale was believed to be separated from the alloy during cooling, allowing oxygen adsorption on the clean alloy surface. Even then, a clear sulfur peak was found by depth profiling immediately beneath the surface adsorbed oxygen.

Fox *et al.*¹⁴ recently also reported a large amount of sulfur near the interface of $\text{Cr}_2\text{O}_3/\text{Cr}$, formed at 950°C , using analytical electron microscopy. Their analysis was made on traverse sections of an oxidized sample; any separated interfaces obviously would not be able to survive these specimen preparation procedures. Although with their technique it is more difficult to assign an exact location of the detected sulfur relative to the interface, their result combined with the Auger analysis presented here indicates clearly that sulfur could indeed be present at an intact scale/metal interface. This sulfur enrichment is more likely to be an accumulation as a result of continued oxidation under a dynamic situation, rather than that of equilibrium segregation, for the charge and size reasons put forth by Grabke *et al.*⁹ However, if most metal/oxide interfaces are non-coherent and resemble high angle grain boundaries, then even equilibrium segregation to such interfaces could still be expected.

Other than sulfur, another impurity, carbon, was also found on the metal surface of the FeCrAl alloy beneath its alumina scale. Surprisingly however, such interfacial carbon was not found on the Ni–25Cr alloy surface beneath its chromia scale, even though this alloy contains about the same amount of carbon impurity (20–30 ppm) as the FeCrAl alloy. Although the segregation of carbon to Ni surfaces is slightly less favorable than that of Fe, and there is a strong orientation dependency in the case of Ni,¹⁵ these minor differences cannot explain why 20 at.% carbon was found at the alumina/FeCrAl interface, while none appeared at the chromia/NiCr interface.

Grabke *et al.*¹⁶ reported that unlike sulfur, whose segregation to a clean Fe surface was independent of bulk concentration and temperature, the segregation of carbon obeyed a Langmuir model, where the carbon coverage

decreased smoothly as the temperature increased. The carbon was reported to occupy surface interstitial sites with a saturation coverage of 0.2 monolayer. Above 800°C and with a bulk carbon concentration of 30 ppm, the surface coverage would drop to be less than 0.06 monolayer.

The 20 at.% level of carbon found in the present study after oxidation at 900°C and above therefore clearly could not be due to equilibrium segregation. Although it is not clear what mechanism might be responsible for the accumulation of carbon at the alumina/FeCrAl interface, the fact that carbon was found at one type of scale/alloy interface but not the other suggests that it may be related to the way the interface is developed as a result of oxide growth. The accumulated carbon along with sulfur had a combined surface concentration of approximately 40 at.%. If an interface could indeed be weakened by the presence of an interfacial impurity such as sulfur, the extra carbon would be expected to make the alumina/FeCrAl interface even weaker.

Removal of surface scales not only allowed chemical analysis of the underlying alloy surface, it also revealed its microstructures. For both the Fe-18Cr-5Al and the Ni-25Cr alloys, the density of interfacial voids at the metal surface was found to increase with higher oxidation temperatures. Although the mechanism of void formation is not clear, part of it may be the result of the compressive stress developed during oxide growth,¹⁷ and part of it may be related to vacancy injection and condensation during oxidation.¹⁸ This latter process should be more important for the cationic grown chromia scale than for the anionic grown alumina scale. From 900° to 1100°C, the scale growth rate increases by at least an order of magnitude for both oxides.¹⁹ Faster growth at the higher temperature could either result in a higher growth stress or introduce a higher flux of vacancies. Both processes would be expected to enhance the interfacial void formation.

For the alumina scale, the higher number of interfacial voids did not affect scale failure. Upon indentation, the scale delaminated uniformly around the indent. All failures took place at the scale/alloy interface, exposing large areas of metal surface which consisted of either voids or oxide-imprinted regions. Although the number of interfacial voids increased with increasing oxidation temperature, the size of the delaminated area was only proportional to the indentation load, not to the temperature at which the scale was formed. Since sulfur and carbon were found everywhere on the metal side of these interfaces, regardless of the oxidation temperature or the interfacial morphology, it seems reasonable that the weakness of the interface was due mainly to the detrimental presence of these impurities. Therefore, by reducing the level of impurities within the alloy, either by using ultra-pure starting materials²⁰ or by mechanically²¹ or chemically²² removing the indigenous impurities, the interface could be strengthened.

Failures of the chromia scales were quite different from that of the alumina scales, even for those of a similar thickness. Upon indentation, the chromia scales preferentially failed at areas above interfacial voids. Larger forces associated with a scratch would uncover some oxide-imprinted regions, but the areas being exposed were comparatively smaller than that found with the alumina scales, and were all next to some voids. The degree of scale failure was closely related to the oxidation temperature. For example, the scales formed at 900°C did not spall during cooling, but that of a similar thickness formed at 1100°C spalled 30%. Failures of the higher temperature scale always took place at the interface, but could occur either at the interface or within the oxide of the lower temperature scale, indicating that this latter interface was at least as strong as the cohesive strength of its oxide. Although the scale fracture behavior may be very different with different oxidation temperatures, the metal surface beneath these scales was always found with an equal amount of sulfur enrichment. It seems then that for this system, the oxide spallation behavior is dominated by the microstructural difference at the interface, which resulted from the oxidation process, and sulfur segregation becomes a secondary effect.

This is not to say that the presence of sulfur at the $\text{Cr}_2\text{O}_3/\text{NiCr}$ interface is unimportant. It may be that the $\text{Cr}_2\text{O}_3/\text{NiCr}$ system has a higher tolerance for sulfur than the $\text{Al}_2\text{O}_3/\text{FeCrAl}$ system, or perhaps the added 20 at.% carbon on the $\text{Al}_2\text{O}_3/\text{FeCrAl}$ interface indeed made a difference between the strength of the two interfaces. The detrimental effect of sulfur on chromia-forming alloys has been reported a few times in recent years. When Rhys-Jones and Grabke²³ deliberately added a high concentration, 0.02%, of sulfur in their Fe-20Cr alloy, the resulting scale did show poorer adherence. Melas and Lees²⁴ found that by hydrogen annealing their chromium specimen prior to oxidation the indigeneous sulfur in the specimen could be removed, and an adherent scale was formed. However, the H_2 -treated chromium also oxidized at least three times slower than the untreated one. Smeggil²⁵ has reported similar behavior with a ultrahigh purity Ni-40Cr alloy, where the clean alloy oxidized slower and developed a very adherent scale. Perhaps in these cases, the final good adhesion of the chromia scale was due to the combined effect of a modified growth and a cleaner interface, in agreement with what is proposed from this work. Although the adverse effect of sulfur on the adhesion of alumina scales may have been substantiated in recent years,²⁶ this effect on chromia scales warrants more careful future studies.

CONCLUSIONS

Results from this study clearly demonstrated that sulfur as an alloying impurity did accumulate at the scale/alloy interface during oxidation. This

is true for alumina as well as for chromia scales which formed between 900°C and 1100°C. The accumulation was found not only on interfacial voids, but also on areas where the scale was in contact with the alloy at temperature. The sulfur concentration was between 17–19 at.% and all of which was located within 4–6 nm from the metal surface. Besides sulfur, approximately 20 at.% carbon was also detected on the FeCrAl surface beneath its alumina scale, but none of this carbon was found at the NiCr surface beneath its chromia scale.

Indentation or scratches always caused alumina scales to separate from the underlying substrate. The degree of decohesion was proportional to the indentation load, but not affected by the oxidation temperature. The chromia scale fractured preferentially above interfacial voids. The scale failure behavior was strongly related to the oxidation temperature where higher temperatures resulted in a higher density of interfacial voids.

For alumina scales, the impurity accumulation at the scale/alloy interface is believed to be the major cause for scale failure. For chromia scales, the dominated effect appeared to be the interfacial morphology which resulted from the oxidation process, whereas impurity accumulation at the interface is only a secondary effect.

ACKNOWLEDGMENT

This work was supported by the Electric Power Institute under Contract No. RP 2261-1, through an agreement with the U.S. Department of Energy under Contract No. DE-AC03-76SF00098.

REFERENCES

1. D. P. Whittle and J. Stringer, *Phil. Trans. Roy. Soc. London* **A27**, 309 (1979).
2. Y. Ikeda, K. Nii, and K. Yoshihara, *Trans. Jpn. Inst. Met. Suppl.* **24**, 207 (1983).
3. A. W. Funkenbusch, J. G. Smeggil, and N. S. Bornstein, *Metall. Trans.* **16A**, 1164–1165 (1985).
4. D. G. Lees, *Oxid. Met.* **27**, 75 (1987).
5. K. L. Luthra and C. L. Briant, *Oxid. Met.* **26**, 397–416 (1986).
6. J. L. Smialek and R. Browning, in *High Temperature Materials Chemistry III*, Z. A. Munir and D. Cubicciotti, eds. (The Electrochem. Soc., Pennington, NJ, 1986), pp. 258–272.
7. J. G. Smeggil and G. G. Peterson, *Oxid. Met.* **29**, 103–119 (1988).
8. C. G. H. Walker and M. M. El Comati, *Appl. Surf. Sci.* **35**, 164–172 (1988/89).
9. H. J. Grabke, D. Wiemer, and H. Viehhaus, *Appl. Surf. Sci.* **47**, 243–250 (1991).
10. P. Y. Hou and J. Stringer, in *Microscopy of Oxidation*, M. J. Bennett and G. W. Lorimer, eds. (Institute of Metals, 1991), p. 1345.
11. S. S. Chiang, D. B. Marshall, and A. G. Evans, in *Surfaces and Interfaces in Ceramic and Ceramic-Metal Systems*, J. Pask and A. G. Evans, eds. (Plenum, New York, 1981), pp. 603–617.
12. J. Valli, *J. Vac. Sci. Technol.* **A4**(6), 3007–3014 (1986).

13. R. M. Cannon, R. M. Fisher, and A. G. Evans, in *Thin Films—Interfaces and Phenomena*, Vol. 54, R. J. Nemanich, P. S. Ho, and S. S. Lau, eds. (MRS Symp. Proc. 1986), pp. 799–804.
14. P. Fox, D. G. Lees, and G. W. Lorimer, *Oxid. Met.* **36**, 491–503 (1991).
15. J. Benard, ed., *Adsorption on Metal Surfaces—An Integrated Approach*, Vol. 13 (Studies in Surface Science and Catalysis, Elsevier, 1983), pp. 55–97.
16. H. J. Grabke, W. Paulitschke, G. Tauber, and J. Viehhaus, *Surf. Sci.* **63**, 377–389 (1977).
17. J. E. Harris, *Acta Metall.* **26**, 1033–1041 (1978).
18. J. Stringer, *Metall. Rev.* **11**, 113–128 (1966).
19. H. Hindam and D. P. Whittle, *Oxid. Met.* **18**, 245–284 (1982).
20. J. G. Smeggil, *Mater. Sci. Eng.* **87**, 261 (1987).
21. J. L. Smialek, in *Corrosion and Particle Erosion at High Temperatures*, V. Srinivasan and K. Vedula, eds. (TMS, 1989), pp. 425–457.
22. D. R. Sigler, *Oxid. Met.* **29**, 23–43 (1988).
23. T. N. Rhys-Jones and H. J. Grabke, *Mater. Sci. Tech.* **4**, 446–454 (1988).
24. I. Melas and D. G. Lees, *Mater. Sci. Tech.* **4**, 455–456 (1988).
25. J. G. Smeggil, *Corrosion and Particle Erosion at High Temperatures*, V. Srinivasan and K. Vedula, eds. (TMS, 1989), pp. 403–424.
26. J. L. Smialek, in *Microscopy of Oxidation*, M. J. Bennett and G. W. Lorimer, eds. (Institute of Metals, 1991), pp. 258–270.